

# THE JOURNAL OF CHEMICAL PHYSICS

VOLUME 53, NUMBER 7

1 OCTOBER 1970

## Three-Body Recombination and Dissociation of Nitrogen: A Comparison between Theory and Experiment\*

VEN H. SHUI, JOHN P. APPLETON, AND JAMES C. KECK

*Massachusetts Institute of Technology, Cambridge, Massachusetts 02139*

(Received 16 April 1970)

The modified phase-space theory of reaction rates is used to calculate the over-all recombination and dissociation rate coefficients of nitrogen in a heat bath of argon atoms. Substantial quantitative agreement is obtained between the theoretical predictions and the low-temperature (90–611°K) "discharge-flow-tube" measurements of the recombination rate coefficient and the high-temperature (8000–15 000°K) "shock-tube" measurements of the dissociation rate coefficient. The success of the theory in correlating the experimental measurements over such a wide temperature range clearly illustrates the importance of the weak attractive forces between the nitrogen and argon atoms for recombination at low temperatures, the marked reduction in the rates at high temperatures due to nonequilibrium distributions in the vibrational state populations of the molecules, and the major contribution to the over-all reaction rate coefficients due to reaction progress via the first electronically excited molecular state of nitrogen over the entire temperature range. The working relationships required for applying the modified phase-space theory to predict the dissociation and recombination rate coefficients of other diatomic molecules in the presence of weakly attracting collision partners, such as argon atoms, are summarized.

### I. INTRODUCTION

The phase-space theory of reaction rates provides the most general method of calculating the reaction rates of atomic and molecular systems whose interaction can be described by the motion of a representative point in the classical phase space of the system. It can be shown that the more conventional classical reaction rate theories such as unimolecular decay theory,<sup>1</sup> absolute reaction rate theory,<sup>2</sup> and available energy theory,<sup>3</sup> are all special cases of the phase-space theory. For a general discussion of these points we refer to Keck.<sup>4</sup>

In this paper we have used the phase-space-theory approach, as developed by Keck<sup>4,5</sup> for three-body reactions, which incorporates the correction due to a nonequilibrium distribution in the vibrational state populations of the molecules, Keck and Carrier,<sup>6</sup> to predict the rates of dissociation and recombination of nitrogen diluted in a large excess of argon. Both the qualitative and quantitative agreement which is demonstrated by a comparison of these theoretical predictions with the low-temperature "discharge-flow-tube" recombination rate measurements due to Campbell and Thrush<sup>7</sup> (196–327°K) and Clyne and Stedman<sup>8</sup> (90–611°K), and with the high-temperature "shock-tube" dissociation measurements (8000–15 000°K)

due to Appleton, Steinberg, and Liguornik,<sup>9</sup> is substantial.

The success of the theory as demonstrated here, which was not apparent in previous attempts<sup>6,9</sup> of comparison with experiment, clearly illustrates the importance of: (1) the weak attractive van der Waals forces between the nitrogen and argon atoms for recombination at low temperatures, (2) the marked reduction in the magnitude of the rate coefficients from their equilibrium values at high temperatures due to nonequilibrium distributions in the vibrational state populations of the molecules, and (3) the major contributions to the over-all reaction rate due to reaction progress via the first electronically excited molecular state,  $N_2(A^3\Sigma_u^+)$ , over the entire temperature range of experiments.

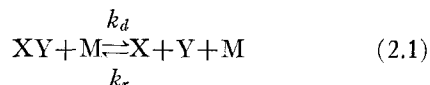
Provided that the total interaction potential of the three-body system can be defined, the modified phase-space theory which we have used here allows computations of the dissociation and recombination rate coefficients to be made which do not contain arbitrary constants and undetermined "steric factors." Thus, when subsequent comparisons are made with reliable experimental measurements, it is usually possible to ascribe any significant disagreement between experiment and theory to inadequacies in the assumed form

of the basic three-body interaction potential. Such comparisons may, therefore, provide a method of making quantitative improvements to the interaction potentials.

We shall not repeat in the following the complete arguments and theoretical development of the phase-space theory which lead to the final expressions for the reaction rate coefficients. Instead, in Sec. II, we shall summarize the working relationships, discuss some of the assumptions embodied in the theory (particularly those relating to the assumed form for the complete three-body interaction potential), and give the prescription for the subsequent calculation of the over-all rate coefficients in which account is taken of the possible influence of electronically excited atomic and molecular states. Section III will be devoted to a brief account of the relevant experimental work. In Sec. IV we shall present our graphical comparisons between the theoretical predictions and the experimental measurements, and Sec. V will contain our concluding discussion.

## II. PHASE-SPACE THEORY OF THREE-BODY REACTION RATES

Here, we are concerned with that class of three-body recombination and dissociation reactions which are commonly written



and are observed to proceed in accordance with the rate equation

$$\begin{aligned} d[\text{XY}]/dt &= -k_d[\text{XY}][\text{M}] + k_r[\text{X}][\text{Y}][\text{M}] \\ &= -d[\text{X}]/dt = -d[\text{Y}]/dt, \end{aligned} \quad (2.2)$$

where  $k_d$  and  $k_r$  are, respectively, the dissociation and recombination rate coefficients. We note that for homonuclear diatomic molecules,  $\text{X}_2$ , the rate equation becomes

$$\begin{aligned} d[\text{X}_2]/dt &= -k_d[\text{X}_2][\text{M}] + k_r[\text{X}]^2[\text{M}] \\ &= -d[\text{X}]/2dt. \end{aligned} \quad (2.3)$$

It is implied by the above rate equations that we restrict our attention to the calculation of reaction rates at times which are long by comparison with any "induction periods," i.e., the time intervals required to achieve close approximations to steady-state distributions in the internal energy states of the molecules and atoms (see, for example, Ref. 10 for a discussion of the induction period due to vibrational relaxation); therefore, both  $k_d$  and  $k_r$  are to be regarded as functions of temperature alone, and their ratio equal to the equilibrium constant, viz.,

$$k_d/k_r = [\text{X}]_e[\text{Y}]_e/[\text{XY}]_e = K(T), \quad (2.4)$$

where the subscript  $e$  denotes the equilibrium concentrations at the temperature  $T$ .

### A. The Barrier Rate Coefficients

The first objective of the phase-space theory is the calculation of what Keck has termed the "barrier rate" coefficients  $k_d^B$  and  $k_r^B$ , which represent rigorous upper bounds to the actual rate coefficients. Since Eq. (2.4) relates these coefficients, it is only necessary to calculate one of them,  $k_r^B$ , say.

The phase-space theory defines these barrier rate coefficients in terms of the total one-way flow of representative points in the classical phase space across a suitably defined surface which separates the initial states of the system, i.e., the reactants, from their final states, i.e., the products.

For three-body reactions the complete system phase space is 18D so that each representative point is defined by nine configuration coordinates,  $q_i$ , and nine momenta,  $p_i$ . However, because the chemical state of a system of three interacting atoms (by which we mean whether they are to be regarded as reactants or products) is independent of their center-of-mass position  $\mathbf{R}$  and momentum  $\mathbf{P}$ , the "working" phase space is reduced to 12 dimensions. The Hamiltonian for this reduced phase space is thus equal to the total three-body potential energy,  $V_0$ , plus the kinetic energies of the three atoms relative to the center of mass.

We shall not repeat Keck's theoretical development of the expression for  $k_r^B$  except to enumerate four primary assumptions. These are:

(1) The internal degrees of freedom of the three-body systems are in local equilibrium on the phase-space surface which separates reactants from products, so that the density of representative points can be described by a Boltzmann distribution, viz.,

$$\rho = \rho_0 \exp(-H/kT), \quad (2.5)$$

where  $H$  is the system Hamiltonian; for the case of an attracting third body, this equilibrium assumption implies a "relaxed complex" (see discussion in Sec. IV).

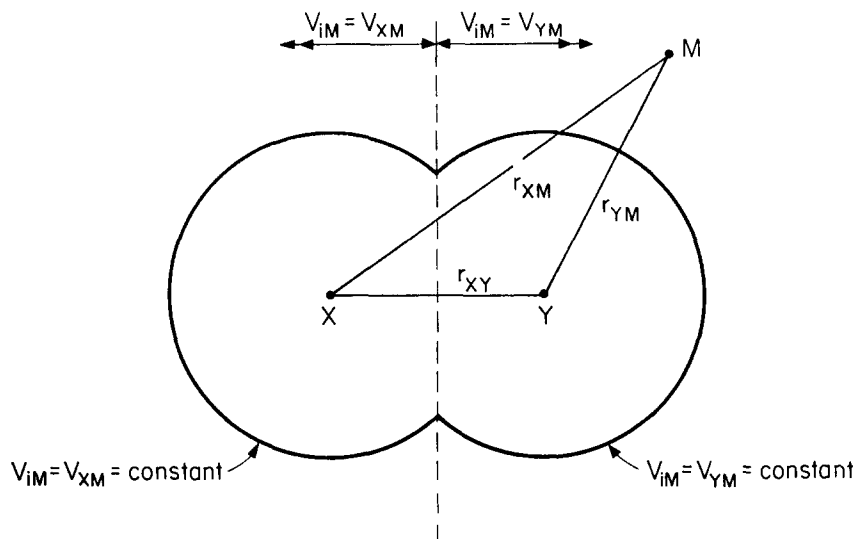
(2) Electronic transitions do not occur during interactions (in accordance with the Born-Oppenheimer separation) so that the three-body interaction potential,  $V_0$ , is invariant.

(3) The three-body interaction potential is given as the sum of two potentials,

$$V_0 = V_{\text{XY}} + V_{i\text{M}}, \quad (2.6)$$

where  $V_{\text{XY}}$  is the potential of the recombining atoms ( $\text{X}-\text{Y}$ ), and  $V_{i\text{M}}$  is the potential between one of the atoms and the third body  $\text{M}$ ;  $V_{i\text{M}} \equiv V_{\text{XM}}$ , when the internuclear distance  $r_{\text{XM}}$  is smaller than  $r_{\text{YM}}$ , and  $V_{i\text{M}} \equiv V_{\text{YM}}$ , when  $r_{\text{XM}} > r_{\text{YM}}$ . A constant energy surface of such a potential is shown in Fig. 1. (Keck<sup>4</sup> has termed this the "dumbbell" model of the interaction potential.)

FIG. 1. The "dumbbell" model for the three-body interaction potential illustrating a constant energy surface.



(4) The surface  $S$  separating reactants from products is defined by the constraints

$$E_{XY} - B_{XY} = 0; \quad E \geq 0, \quad (2.7)$$

where  $E$  is the total internal energy of the three-body system (X-Y-M),  $E_{XY}$  is the internal energy of the recombining atoms (X-Y), and  $B_{XY}$  is the height of the rotational barrier [the effective potential-energy diagram for the system (X-Y), together with a projection of the barrier surface  $S$  are shown in Fig. 2]. In this paper we have used the Morse potential function,

$$V(r) = U \{ [1 - \exp[-\beta(r - r_e)]]^2 - 1 \}, \quad (2.8)$$

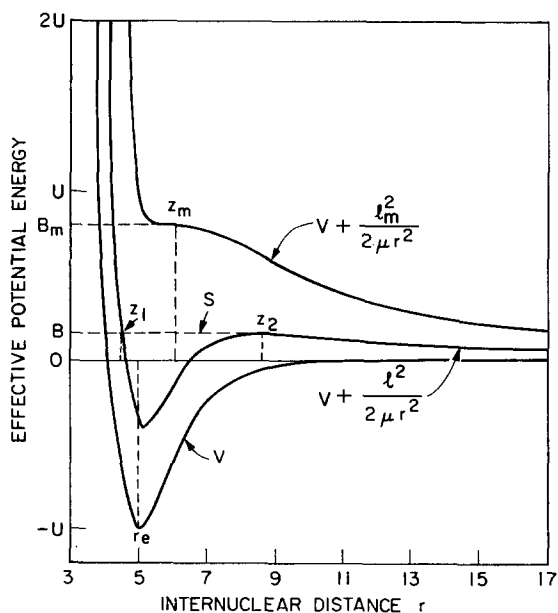


FIG. 2. Effective Morse potential-energy curves for the molecule XY illustrating the projection of the Barrier surface  $S$ . The symbol  $l$  denotes the angular momentum of the molecule.

to represent both  $V_{XY}$  and  $V_{iM}$  with appropriate suffices added to the potential parameters  $U$ ,  $\beta$ , and  $r_e$  to identify the particular two-body potential under consideration.

Keck's final expression for the barrier rate coefficient,  $k_r^B$ , may be written in the form

$$k_r^B = 4\pi^2 f a^2 z_2^2 (z_2 - z_1) (8kT / \pi \mu_{XY})^{1/2} \times [1 - \exp(-B_m/kT)], \quad (2.9)$$

where  $f = g_{XY} / g_X g_Y$  is the electronic degeneracy factor,  $a$  is the effective collision radius,  $\mu_{XY} = m_X m_Y / (m_X + m_Y)$  is the reduced mass of the molecule XY, and  $B_m$  is the *maximum* height of the rotational barrier. The characteristic distance  $z_2$ , defined by Eq. (2.12) below, is the position of the rotational barrier on the effective potential-energy curve which is most favorable for reaction at a given temperature, and  $z_1$  is the corresponding inner turning point shown in Fig. 2.

For the purpose of providing a simple physical explanation for the form of Eq. (2.9), we may point out that the factor  $4\pi z_2^2 (z_2 - z_1)$  is a molecular volume proportional to the number of atom pairs (X-Y), close enough to recombine, whereas the factor  $\pi a^2 (8kT / \pi \mu_{XY})^{1/2}$  is a rate constant proportional to the frequency at which the (X-Y) pairs are stabilized under the influence of the third body M. The reason for the appearance of the reduced mass,  $\mu_{XY}$ , for the recombining atoms in the velocity term rather than the reduced mass,  $\mu_{XY,M}$ , for the collisions of (X-Y) with M, is that in the "barrier rate" it is the rate of momentum transfer from M to (X-Y), rather than the collision rate of M with (X-Y), which controls the recombination. The additional factor  $[1 - \exp(-B_m/kT)]$  simply eliminates those atom pairs which cannot form bound molecules because of their excessive orbital angular momentum.

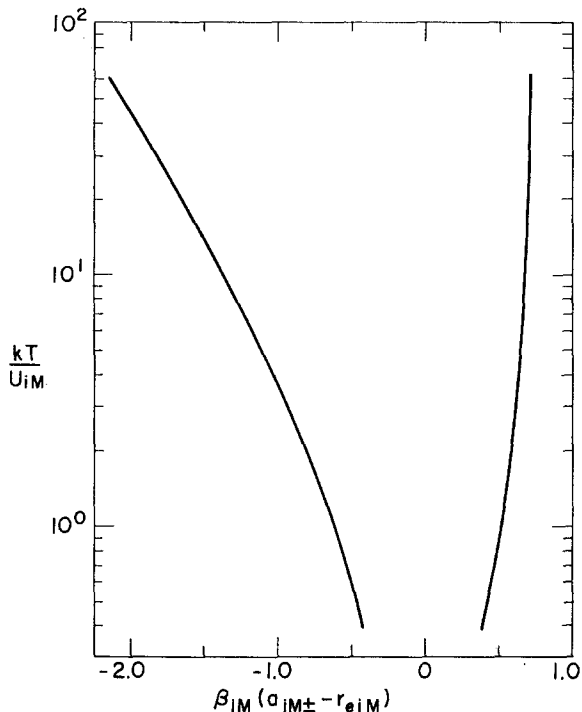


FIG. 3. Graphical solution of Eq. (2.11) illustrating the variation of  $a_{iM\pm}$  as a function of  $T$  for a Morse potential.

The square of the effective collision radius,  $a^2$ , may be approximated by the expression

$$a^2 = 2^{-3/2} \left\{ \frac{m_Y}{m_X + m_Y} \left[ a_{XM-}^{-2} \exp\left(\frac{U_{XM}}{kT}\right) + a_{XM+}^{-2} \right. \right. \\ \left. \left. \times \exp\left(\frac{U_{XM}}{kT}\right) - a_{XM+}^{-2} \right] + \frac{m_X}{m_X + m_Y} \right. \\ \left. \times \left[ a_{YM-}^{-2} \exp\left(\frac{U_{YM}}{kT}\right) + a_{YM+}^{-2} \exp\left(\frac{U_{YM}}{kT}\right) - a_{YM+}^{-2} \right] \right\}, \quad (2.10)$$

where  $a_{iM\pm}$  are given by the larger ( $a_{iM+}$ ) and smaller ( $a_{iM-}$ ) finite positive roots of the equation

$$\left\{ \frac{d}{dr_{iM}} \left[ \left| \frac{dV_{iM}}{dr_{iM}} \right| \exp\left(\frac{-V_{iM}}{kT}\right) \right] \right\}_{r_{iM}=a_{iM\pm}} = 0 \\ (i=X, Y). \quad (2.11)$$

The graphical solution of Eq. (2.11) is illustrated in Fig. 3 for the case of a Morse potential.

The position of the rotational barrier,  $z_2$ , is approximately given by the root of the equation

$$\left\{ \frac{d}{dz} \left[ \left( \frac{dB}{dz} \right) \exp(-B/kT) \right] \right\}_{z=z_2} = 0, \quad (2.12)$$

where

$$B = V_{XY}(z) + \frac{1}{2} z \left[ \frac{dV_{XY}(z)}{dz} \right] \quad (z_m \leq z \leq +\infty) \quad (2.13)$$

is the equation for the rotational barrier height, and the inner turning point,  $z_1$ , is determined from the equation

$$B(z_2) = V_{XY}(z_1) + [B(z_2) - V_{XY}(z_2)](z_2/z_1)^2. \quad (2.14)$$

Graphical solutions of Eqs. (2.12) and (2.14) for a family of Morse potentials, which are characterized by the parameter  $\beta r_e$ , are illustrated in Fig. 4.

### B. Statistical Trial Corrections

The barrier rate coefficient, as defined by Eq. (2.9), only yields an upper bound for the rate of recombination. The reason is that although in principle there exists in the phase space a class of surfaces which are crossed only once by any one representative point trajectory, in practice, the "trial" surface chosen (i.e., the "barrier" surface) will almost never belong to this class and may be crossed many times by single trajectories. Keck<sup>12</sup> has developed an efficient statistical method for investigating this effect. The procedure involves the random sampling of phase-space trajectories which cross the "trial" surface (in particular, the "barrier" surface) and numerical integration of the classical equations of motion in both timewise directions to determine the complete trajectories. Thus, the number of crossings of the "trial" surface and hence the number of completed reactions can be determined.

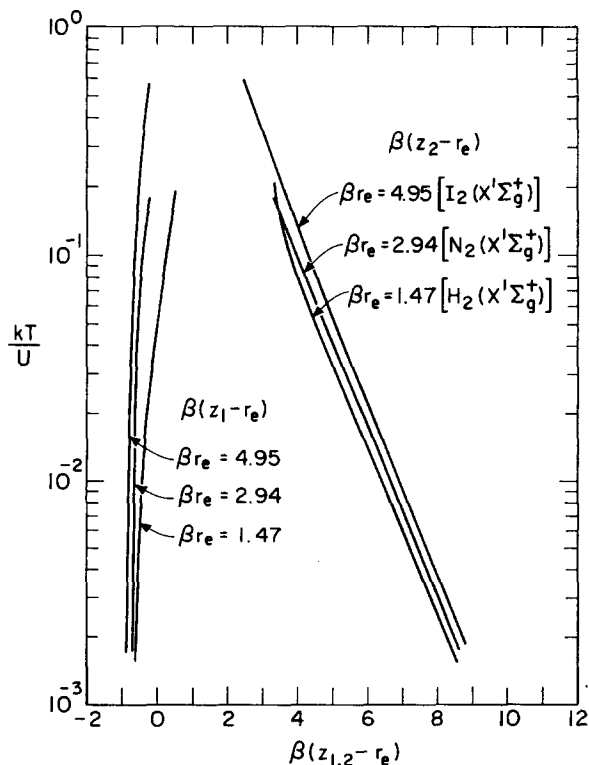


FIG. 4. Graphical solution of Eqs. (2.12) and (2.14) illustrating the variation of  $z_{1,2}$  as a function of  $T$  for variety of Morse potentials.

A plot of  $(N/N_0)$  versus  $[\mu_{XY}/(\mu_{XY,M} + \mu_{XY})]$ , where  $N$  is the number of complete reaction trajectories and  $N_0$  is the total number of trajectories sampled, can be found in Ref. 12. Alternatively, Keck<sup>4</sup> has given a semiempirical correlation formula for  $(N/N_0)$  in the form

$$N/N_0 = \frac{1}{3}[4 - \exp(-4\chi/5)] \exp(-4\chi/5), \quad (2.15)$$

where

$$\chi = (\mu_{XY,M}/\mu_{XY})^{1/2} \quad (2.16)$$

and

$$\mu_{XY,M} = m_M(m_X + m_Y)/(m_X + m_Y + m_M). \quad (2.17)$$

The value of  $(N/N_0)$  thus obtained has been used in this paper as a statistical correction factor which multiplies the values of  $k_r^B$  given by Eq. (2.9). It should be pointed out, however, that in Ref. 12 the potentials  $V_{iM}$  were taken to be purely repulsive. Therefore, further work is needed to investigate the possible effects of the weak attractive potential well on the statistical correction factors.

### C. Nonequilibrium Correction

Equilibrium distributions of the energy states have been assumed in the theory so far discussed. However, every process in a gaseous system proceeding at a finite rate involves a perturbation of the equilibrium distribution functions. The thermal dissociation (and recombination) of molecules has been found to proceed by way of intermediate vibrationally excited states, and nonequilibrium distributions in the vibrational energy can have an appreciable effect on the kinetic processes.<sup>13</sup>

The coupled vibration-dissociation-recombination process for a dilute mixture of diatomic molecules in a heat bath of inert atoms has been studied by Keck and Carrier.<sup>6</sup> It was found that for either dissociation or recombination, the relaxation process starts with an initial fast transient, having a duration of the order of the vibrational relaxation time. During the transient period, there is negligible chemical reaction but the population of the vibrational levels approaches a distribution which is extremely close to a solution of the steady-state master equations (i.e., a distribution in which the relative populations of the vibrational levels do not change with time). This transient is followed by a very much slower phase where the steady-state distribution is maintained and the chemical reaction proceeds to equilibrium.

For dissociation, the steady-state distribution is very nearly Boltzmann except near the dissociation limit (within a few  $kT$  of the dissociation limit) where the levels are underpopulated; for recombination, the steady-state distribution is Boltzmann near the dissociation limit but the lower levels are underpopulated. Because of this, the steady-state rate coefficients  $k_r$  and  $k_d$  are smaller than the corresponding equilibrium rate coefficients  $k_{re}$  and  $k_{de}$ , although the ratio of the

rate coefficients is very nearly equal to the equilibrium constant, i.e.,

$$k_d/k_r = k_{de}/k_{re} = K_c(T). \quad (2.18)$$

By assuming a classical Morse oscillator to represent the molecule, Keck and Carrier solved the appropriate master equation to give the following result:

$$k/k_e = k_r/k_{re} = k_d/k_{de} = [2R(\delta)S(\delta) + \frac{1}{2}]^{-1}, \quad (2.19)$$

where

$$2R(\delta)S(\delta) = \left( \frac{3 \exp(4\gamma/9) H_\gamma \{ (8\gamma/9)^{1/2} \}}{4 - \exp(-8\gamma/9)} \right) \times \left( \frac{1 + (4\gamma/9\delta)^{1/2}}{1 - (4\gamma/9\delta)^{1/2}} \right), \quad (2.20)$$

$$H_\gamma \{t\} = \frac{4}{3}(\pi\gamma)^{1/2} \operatorname{erf}\{t\} + \exp(-t^2/2), \quad (2.21)$$

$$\operatorname{erf}\{t\} = (2\pi)^{-1/2} \int_{-\infty}^t \exp\left(-\frac{x^2}{2}\right) dx, \quad (2.22)$$

$$\gamma = \left(\frac{1}{3}\pi\beta L\right)^2 \mu_3/\mu_{12} \quad (2.23)$$

is the "adiabaticity" parameter,  $\beta_{XY}$  is the usual Morse potential parameter [see Eq. (2.8)],  $\delta$  is the reciprocal of the dimensionless temperature  $U_{XY}/kT$ , and  $L$  is the range of the interaction potential  $V_{iM}$ . Equation (2.20) incorporates a correction for an error which appeared in the original version of the paper by Keck and Carrier,<sup>6</sup> see Ref. 9.

We now recognize that the barrier rate  $k_r^B$ , given by Eq. (2.9), is actually composed of four parts,

$$k_r^B = k_{rX+}^B + k_{rX-}^B + k_{rY+}^B + k_{rY-}^B, \quad (2.24)$$

corresponding to contributions to the rate from four distinctly different configurations of the three-body collision complex. Each configuration corresponds to a maximum in the rate of momentum transfer between (X-Y) and M, which has an associated separation distance  $a_{iM\pm}$ , between one of the recombining atoms (X or Y) and the collision partner M, see Eq. (2.11). For each component of  $k_r^B$  we obtain the ratios  $(k/k_e)$  from Eq. (2.19), which are then used in this paper as the nonequilibrium correction factors which multiply the corresponding components of  $k_r^B$ . Thus,

$$k_r(m | p, q) = \left[ k_{rX+}^B \left(\frac{k}{k_e}\right)_{X+} + k_{rX-}^B \left(\frac{k}{k_e}\right)_{X-} + k_{rY+}^B \right. \\ \left. \times \left(\frac{k}{k_e}\right)_{Y+} + k_{rY-}^B \left(\frac{k}{k_e}\right)_{Y-} \right] \frac{N}{N_0}, \quad (2.25)$$

where  $k_r(m | p, q)$  is the rate coefficient for the recombination of atoms in electronic states  $p$  and  $q$ , to molecules in electronic state  $m$  (see Fig. 5 and Sec. II.D for an explanation of our notation),  $(N/N_0)$  is the statistical correction factor, and  $(k/k_e)_{i\pm}$  are the nonequilibrium correction factors given by Eq. (2.19).

In Ref. 6, an exponential interaction potential having

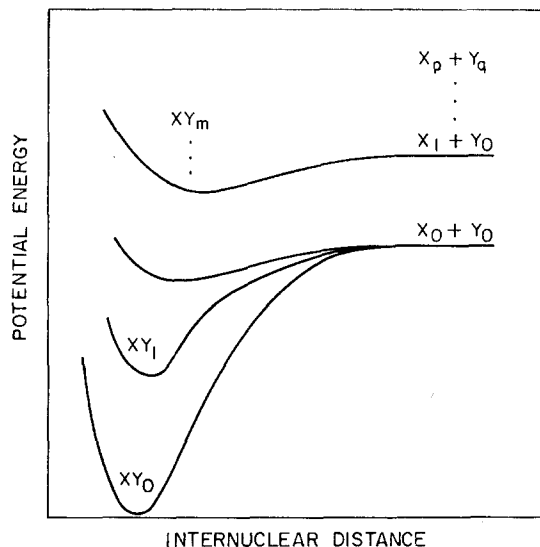


FIG. 5. Illustration of typical diatomic molecule potential-energy curves for a number of different electronic states of the molecule and atoms.

the form  $V_{iM} = V_e \exp(-r/L_{iM})$  was used. The range  $L_{iM}$  has been given by Mason and Vanderslice<sup>14</sup> as

$$L_{iM} = 2^{1/2} a_0 I_H / (I_i + I_M) \quad (i = X, Y), \quad (2.26)$$

where  $a_0$  is the Bohr radius,  $I_H$  is the ionization potential of hydrogen,  $I_i$  and  $I_M$  are the ionization potentials of the interacting atoms, and the empirical rule of the geometric mean for potentials, i.e.,  $V_{iM} = (V_{ii} V_{MM})^{1/2}$ , has been used.

Herzfeld and Litovitz<sup>15</sup> fitted  $V_{iM}$  to a Lennard-Jones (6-12) potential and found that the range  $L = 0.20 \pm 0.04 \text{ \AA}$  for a number of molecular collisions. However, they also concluded that the slope of the repulsive part of the Lennard-Jones (6-12) potential curve was too steep for  $V_{iM}/U_{iM} \gg 1$ , where  $U_{iM}$  is the potential well depth. This is in agreement with the recent measurements of Jordan, Colgate, Amdur, and Mason,<sup>16</sup> who deduced:  $V_{\text{NAr}} = 114 r_{\text{NAr}}^{-6.37} \text{ eV}$  for  $1.99 \text{ \AA} < r_{\text{NAr}} < 2.49 \text{ \AA}$ . Parenthetically, it is encouraging to note that the range  $L_{\text{NAr}}$ , determined by plotting  $\ln V_{\text{NAr}}$  versus  $r$  using the above power-law expression, is  $0.326 < L_{\text{NAr}} < 0.348 \text{ \AA}$ , whereas the value given by Eq. (2.26) is  $0.336 \text{ \AA}$ .

In our calculations, we have matched the slopes of the exponential form for the potential  $V_{iM}$  to a Morse potential [Eq. (2.8)] which we use to describe the interaction between nitrogen and argon atoms. The matching points were taken to be  $r_{iM} = a_{iM\pm}$ , see Eq. (2.11), Fig. 6, and Sec. IV.

#### D. Contributions from Electronically Excited Molecular and Atomic States

The contributions to the over-all rate coefficients due to reaction progress via electronically excited molecular states may be important in certain cases;

two such possible cases are discussed in Secs. III.A and III.C. Therefore, we must develop some means of correlating the calculated individual recombination rate coefficients with the experimentally measured recombination or dissociation rate coefficients.

By considering that the molecules and atoms may exist in their allowable electronic states which we identify by the suffix  $m$  for molecules so that  $\text{XY}_{m=0}$  is the ground molecular state,  $\text{XY}_{m=1}$  is the first excited state, etc., and likewise, identify the atomic states by the suffices  $p$  and  $q$  as illustrated by the potential-energy curves in Fig. 5, we may write the rate equation for the over-all reaction (2.1) in the form

$$\begin{aligned} \partial[\text{XY}]/\partial t &= \sum_m \partial[\text{XY}_m]/\partial t \\ &= - \sum_m k_d(m | p, q) [\text{XY}_m][\text{M}] \\ &\quad + \sum_m k_r(m | p, q) [\text{X}_p][\text{Y}_q][\text{M}] \\ &= - \sum_p \partial[\text{X}_p]/\partial t = - \sum_q \partial[\text{Y}_q]/\partial t. \end{aligned} \quad (2.27)$$

We note that as a consequence of the Born-Oppenheimer separation, the specification of a particular molecular state automatically identifies the atomic states. By comparing Eq. (2.27) with Eq. (2.2) we thus obtain the following expressions for the over-all rate coefficients in terms of the individual rate coefficients,

$$k_a = \sum_m k_d(m | p, q) [\text{XY}_m] / [\text{XY}] \quad (2.28)$$

and

$$k_r = \sum_m k_r(m | p, q) [\text{X}_p][\text{Y}_q] / [\text{X}][\text{Y}]. \quad (2.29)$$

Now in order to determine the steady-state distribu-

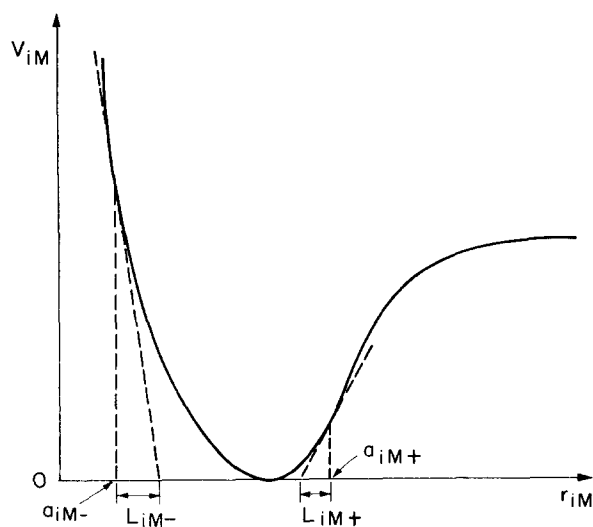
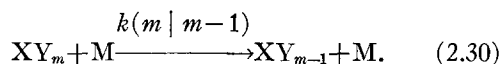


FIG. 6. Effective ranges  $L_{iM-}$  and  $L_{iM+}$  for a Morse potential-energy curve at separations  $a_{iM-}$  and  $a_{iM+}$ , respectively. The ranges are obtained by matching the slopes of the exponential form of the potential  $V_{iM}$  to the Morse potential at the corresponding separations.

tions  $[XY_m]/[XY]$ , etc., it is necessary to know the ratios of the rate coefficients  $k_d(m|p, q)/k(m|m-1)$ , etc., where  $k(m|m-1)$  is the rate coefficient for the de-excitation reaction,



Generally, these rates are not known and therefore, in the same spirit which is adopted in calculating the barrier rate coefficients of dissociation and recombination between individual electronic states of the molecules and atoms, we shall assume that each electronic state of a particular species is present in the reacting system in its equilibrium proportion relative to the total concentration of that species. By making this assumption, the rate coefficients which we calculate will be upper bounds for the over-all rate coefficients and thus will only be realized experimentally if there are reaction paths which allow the excited states to equilibrate rapidly (see Sec. III.C). Thus we set

$$[XY_m]/[XY] = Q_m / \sum_m Q_m, \quad (2.31)$$

etc., where  $Q_m$  is the total particle partition function of the molecule  $XY_m$  in the electronic state  $m$ . Therefore,

$$k_d = \sum_m k_d(m|p, q) Q_m / \sum_m Q_m \quad (2.32)$$

and

$$k_r = \sum_m k_r(m|p, q) Q_p Q_q / \sum_p \sum_q Q_p Q_q. \quad (2.33)$$

It is to be noted that because of detailed balancing,

$$k_d(m|p, q) / k_r(m|p, q) = Q_p Q_q / Q_m, \quad (2.34)$$

we have

$$k_d = \sum_m k_r(m|p, q) Q_p Q_q / \sum_m Q_m, \quad (2.35)$$

so that

$$k_d / k_r = \sum_p \sum_q Q_p Q_q / \sum_m Q_m, \quad (2.36)$$

which is the equilibrium constant based on total concentrations.

Now in many of the dissociation and recombination rate experiments reported in the literature, the rate coefficients are based on measurements of the rate of disappearance (or appearance) of a single electronic state of a particular reacting species. Furthermore, this state is often the ground electronic state, for instance, in the high-temperature shock wave dissociation measurements of nitrogen due to Appleton *et al.*,<sup>9</sup> it was the rate of disappearance of the ground state,  $X^1\Sigma_g^+$ , which was measured. However, even at such high temperatures, by far the greatest proportion of the molecules were present in the ground state since  $Q(X^1\Sigma_g^+) \gg Q(A^3\Sigma_u^+)$ , etc. Therefore, it may be assumed to a good approximation that

$$k_d = \sum_m k_d(m|p, q) Q_m / Q_{m=0}. \quad (2.37)$$

The corresponding high-temperature recombination rate coefficient is obtained by dividing Eq. (2.37) by Eq. (2.36),

$$k_r = \sum_m k_d(m|p, q) Q_m / \sum_p \sum_q Q_p Q_q. \quad (2.38)$$

If, in addition, it is true that  $Q_{p=0} \gg Q_{p>0}$ , so that the major fraction of the atoms are formed and remain present in their ground electronic state, then

$$k_d = \sum_m k_d(m|0, 0) Q_m / Q_{m=0} \quad (2.39)$$

and

$$\begin{aligned} k_r &= \sum_m k_r(m|0, 0) \\ &= \sum_m k_d(m|0, 0) Q_m / Q_{p=0} Q_{q=0}, \end{aligned} \quad (2.40)$$

so that

$$k_d / k_r = Q_{p=0} Q_{q=0} / Q_{m=0}. \quad (2.41)$$

Although Eq. (2.40) is undoubtedly a good approximation for the over-all recombination rate coefficient at low temperatures where the concentration of excited state atoms is negligible, it is as well to check that the assumption:  $Q_{p=0} \gg Q_{p>0}$ , is justified before using the equilibrium constant defined by Eq. (2.41), to deduce high-temperature recombination rate coefficients from measured dissociation rates in any attempt to compare high- and low-temperature data. For example, the use of the equilibrium constant defined by Eq. (2.41) to deduce the high-temperature recombination rate coefficient from the measured dissociation rate coefficient for the  $N_2$ -Ar system, results in an overestimate of 5% in  $k_r$  at  $10^4$  °K and 12% at  $2 \times 10^4$  °K. However, in view of the other approximations involved, we have used Eqs. (2.40) and (2.41) in this paper.

### III. MEASUREMENTS OF NITROGEN DISSOCIATION AND RECOMBINATION

The experimental measurements of the three-body recombination and dissociation rates of nitrogen, which we have used here for comparison with the theoretical predictions of the phase-space theory, were suggested in the recent review article by Kaufman.<sup>17</sup>

#### A. Low-Temperature Recombination Rate Measurements

It appears that the value for the room-temperature ( $\sim 298$ °K) rate coefficient for the reaction



has been established with some certainty to lie within the range  $3.5$ – $4.1 \times 10^{-33}$   $\text{cm}^6 \text{sec}^{-1}$ .

We have chosen to make particular comparisons with the measurements of Campbell and Thrush<sup>7</sup> and

Clyne and Stedman,<sup>8</sup> primarily because these investigators made measurements of  $k_r$  over a fairly wide temperature range about room temperature. Although Clyne and Stedman's measurements were obtained using pure nitrogen (i.e., they did not use argon as a diluent), their results do cover the wider temperature range (90–611°K), and Campbell and Thrush were unable to detect any difference in their measurements between the efficiency of N<sub>2</sub> and Ar as third-body collision partners.

Both of these investigations used the "discharge-flow-tube" technique in which small concentrations of nitrogen atoms in the ground electronic state, N(<sup>4</sup>S), were produced upstream of the flow tube by means of a low-power continuous radio-frequency discharge. The rate of disappearance of the nitrogen atoms downstream of the discharge was determined by the photometric method of nitric oxide titration.

Campbell and Thrush's work had an additional interest because, on the basis of their Lewis-Raleigh afterglow intensity measurements, they convincingly argued that it is the first excited state of the molecule, N<sub>2</sub>(A <sup>3</sup>Σ<sub>u</sub><sup>+</sup>), which is largely responsible for populating the B <sup>3</sup>Π<sub>g</sub> state via collisions, and not the shallow <sup>5</sup>Σ<sub>g</sub><sup>+</sup> state. Furthermore, on the basis of the observed higher quenching efficiency by N<sub>2</sub>, relative to He or Ar, of the afterglow intensity and the observed pressure dependence of the radiative lifetime of the B <sup>3</sup>Π<sub>g</sub> state, determined by Jeunehomme and Duncan,<sup>18</sup> they concluded that about 50% of the nitrogen-atom recombination in the gas phase passed through the B <sup>3</sup>Π<sub>g</sub> state. Therefore, by assuming their afterglow mechanism to be correct, it would appear that at least 50% of the nitrogen atoms were removed in the gas phase by direct recombination into the A <sup>3</sup>Σ<sub>u</sub><sup>+</sup> state. As we shall show, this conclusion is consistent with our prediction that the rate coefficient for recombination to the first excited state is about twice as large as that for recombination to the ground state.

### B. High-Temperature Dissociation Rate Measurements

The high-temperature dissociation rate measurements which we use for comparison were obtained from shock-tube investigations. The earlier results, due to Byron<sup>19</sup> and Cary,<sup>20</sup> were determined by interferometric measurements of the density variation, caused by dissociation, in the relaxation region immediately following the primary shock wave. It is the present authors' opinion that such interferometric methods are subject to a greater uncertainty of interpretation than the more direct methods which use either light absorption or light emission by the reacting species.

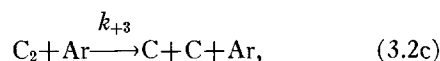
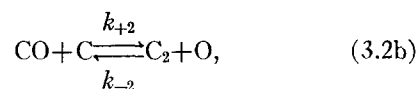
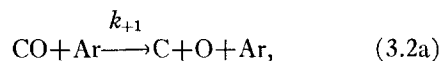
Appleton, Steinberg, and Liquornik<sup>9</sup> used vacuum-ultraviolet light absorption at 1176 Å to monitor the disappearance of ground-state nitrogen molecules in the relaxation region behind reflected shock waves.

Their results, presented in the usual Arrhenius plot, were obtained using mixtures of nitrogen and argon in which the initial mole fraction of nitrogen was varied from 0.02 to 0.2, and covered the temperature range 8000–15 000°K. The values of the dissociation rate coefficients obtained in this study were between a factor of 2 and 3 below Byron and Cary's values. This difference could possibly be explained by different degrees of purity in the test gases but, perhaps, more important is the fact that the relatively small scatter of their data points allowed Appleton *et al.* to determine the temperature dependence of the rate coefficient with more precision than could be done in the previous investigations.

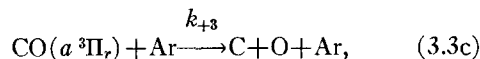
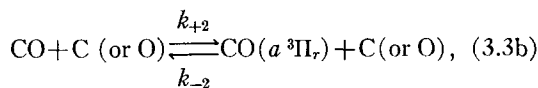
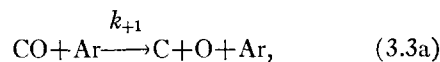
The results of both the low-temperature recombination studies and the high-temperature dissociation studies, referred to above, will be presented graphically in Sec. IV.

### C. Evidence for Excited-State Participation in Dissociation

In two recent shock-tube studies of the dissociation of carbon monoxide by Fairbairn<sup>21</sup> and Appleton, Steinberg, and Liquornik,<sup>22</sup> an induction time was observed in the region immediately following the shock waves. During this induction time little or no dissociation took place, and it was observed to last for periods between 5 and 100 times longer than the characteristic vibrational relaxation time. It was suggested that the induction period was a measure of the time required to build up a steady-state concentration of some intermediate molecular species; the two prime candidates being either C<sub>2</sub> or an excited electronic state of CO (possibly the first excited state, *a* <sup>3</sup>Π<sub>r</sub>). It was not possible to determine from the results of either investigation which of these two intermediates was the most important. However, an analysis of either of the proposed reaction mechanisms:



or



where, during the major portion of the induction period,



$t < \tau$ , it is tacitly assumed that

$$d[\text{C}]/dt \simeq k_{+1}[\text{CO}][\text{M}] \quad (3.4)$$

and

$$d[\text{C}_2]/dt \simeq k_{+2}[\text{CO}][\text{C}] \quad (3.5)$$

or

$$d[\text{CO}(a^3\Pi_r)]/dt \simeq k_{+2}[\text{CO}][\text{C}] \quad (3.6)$$

can be shown<sup>22</sup> to yield an induction time behavior which has the form

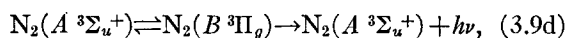
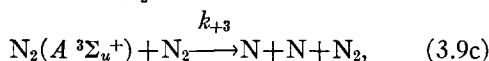
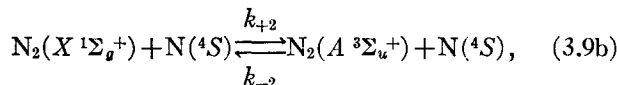
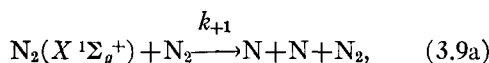
$$\tau^{-1} \alpha (k_{+1} k_{-2} [\text{CO}][\text{Ar}])^{1/2}. \quad (3.7)$$

The induction time measurements of both investigations were in excellent agreement and were very well correlated by the above formula. Indeed, the results indicated that

$$k_{+1} k_{-2} \alpha \exp[-(11.0 \pm 0.3 \text{ eV})/kT] \quad (3.8)$$

over the approximate temperature range 6000–11 000°K. In view of the anticipated weak temperature dependence of  $k_{-2}$  and the fact that the dissociation energy of  $\text{CO}(X^1\Sigma_g^+)$  is 11.1 eV, this result appears to be very satisfactory.

The results of the above carbon monoxide dissociation studies prompted Appleton *et al.* to re-examine their earlier nitrogen dissociation measurements for any evidence of an induction time. Unfortunately, none was found. However, it was noted that in some earlier shock-tube studies of the collisional excitation of the nitrogen first positive emission reported by Wray,<sup>23</sup> evidence for the existence of an induction time is found. Wray observed that the intensity of the first positive emission in the spectral region 6600–8000 Å, increased from zero at the shock front, reached a peak value, and then decayed in an exponential-like fashion during the approach to equilibrium dissociation. A recent re-evaluation of these measurements<sup>24</sup> shows that Wray's measurements of the times to reach the peak intensity were considerably longer than the characteristic vibrational relaxation time. An analysis of the proposed kinetic mechanism



in which similar assumptions as were used above regarding the relative magnitudes of the rate coefficients are made, yields

$$\tau^{-1} \alpha (k_{+1} k_{-2} [\text{N}_2]^2)^{1/2}. \quad (3.10)$$

This induction time formula has been shown to adequately correlate Wray's "time-to-peak-intensity" measurements. Furthermore, the experimental cor-

relation suggests

$$k_{+1} k_{-2} \alpha \exp[-(9.8 \pm 0.5 \text{ eV})/kT] \quad (3.11)$$

over the approximate temperature range 7000–14 000°K. Again, in view of the anticipated weak temperature dependence of  $k_{-2}$  and the fact that the dissociation energy of  $\text{N}_2(X^1\Sigma_g^+)$  is 9.76 eV, it appears that the contribution to the steady-state rate of dissociation of  $\text{N}_2$  via the first excited state may not be unimportant, even though the concentration of the excited state is always very much less than the ground-state concentration of the molecules. As we shall show, this observation is also consistent with our prediction that the effective rate coefficient for dissociation from the first excited state is about twice as large as that for dissociation from the ground state. Evidence to support our implied contention that Reaction (3.9b) can represent a rapid path for populating the  $A^3\Sigma^+$  state, even in the early part of the relaxation region behind shock waves where the atom concentrations are much less than the molecule concentrations, has been deduced using the results of Wray's<sup>23</sup> investigation. We shall report on this re-evaluation of Wray's measurements separately.

#### IV. CALCULATIONS AND RESULTS

The parameters for the Morse potential which describe the interactions between N and Ar atoms are not available from direct experimental data. However, based on experimental results for other systems of atom-atom combination, Bernstein and Muckerman<sup>25</sup> suggested the empirical rule

$$r_e = r_i + r_j + 2.0(\text{\AA}) \quad (4.1)$$

for estimating the equilibrium internuclear separation distance,  $r_e$ . In Eq. (4.1),  $r_i$  and  $r_j$  are the radii of the principal maxima in the radial distribution functions for ground-state atoms  $i$  and  $j$ , calculated by Waber and Cromer<sup>26</sup> following Slater's procedures<sup>27</sup> using relativistic wavefunctions. In order to obtain an estimate for the potential well depth,  $U_{\text{NAr}}$ , we followed the procedure suggested by Bernstein and Muckerman<sup>25</sup> who applied the Badger-Johnston relation<sup>28</sup> to the various molecular-beam scattering data by plotting  $r_e$  versus  $\log U$ ; they found quantitative agreement.

The remaining Morse potential parameter,  $\beta_{\text{NAr}}$ , was obtained by setting  $2\beta_{\text{NAr}} = 1/L_{\text{NAr}}$  where  $L_{\text{NAr}}$  is the range given by Eq. (2.26). We note that the Morse potential curve determined by these parameters has effective ranges  $L_{\text{NAr}} \sim 0.2 \text{\AA}$  for  $V_{\text{NAr}}/U_{\text{NAr}} \sim 1$ , and  $L_{\text{NAr}} \rightarrow 0.33 \text{\AA}$  for  $V_{\text{NAr}}/U_{\text{NAr}} \gg 1$  (see Sec. II.C).

The pertinent spectroscopic data for  $\text{N}_2$  molecules were taken from Gilmore.<sup>29</sup> The values of the parameters required in the calculation of  $k_r$  for the nitrogen/argon system, estimated from the empirical rules mentioned above, are summarized in Table I.

TABLE I. Parameters used for calculating  $k_r$ .

Molecular state	Dissociation products	Equilibrium separation $r_e$ (Å)	Dissociation energy $U$ (eV)	Electronic degeneracy factor $g_{N_2}/g_{N}g_N$	Vibrational energy spacing $\omega$ (cm <sup>-1</sup> )
Spectroscopic data for N <sub>2</sub>					
$X^1\Sigma_g^+$	$^4S+^4S$	1.098	9.756	1/16	2358.1
$A^3\Sigma_u^+$	$^4S+^4S$	1.287	3.589	3/16	1460.6
Interaction potential parameters (N-Ar)					
	$r_c$ (Å)	$U$ (°K)	$\beta$ (Å <sup>-1</sup> )		
	3.18	200	1.49		
Statistical correction factor: $(N/N_0) = 0.32$					

The data listed in Table I were first used to calculate the recombination rate coefficients. The results are shown in Fig. 7, where  $\log k_r$  is plotted versus  $\log T$ . The lower dashed curve shows the variation of  $k_r^B(X^1\Sigma_g^+ | ^4S, ^4S)(N/N_0)$ ; the upper dashed curve repre-

sents the sum of the contributions from both the ground state and the first excited state, ( $A^3\Sigma_u^+$ ), and the solid curve illustrates the effect of incorporating the nonequilibrium correction factors,  $(k/k_e)$ , into the calculation. The important experimental results are also shown for comparison.

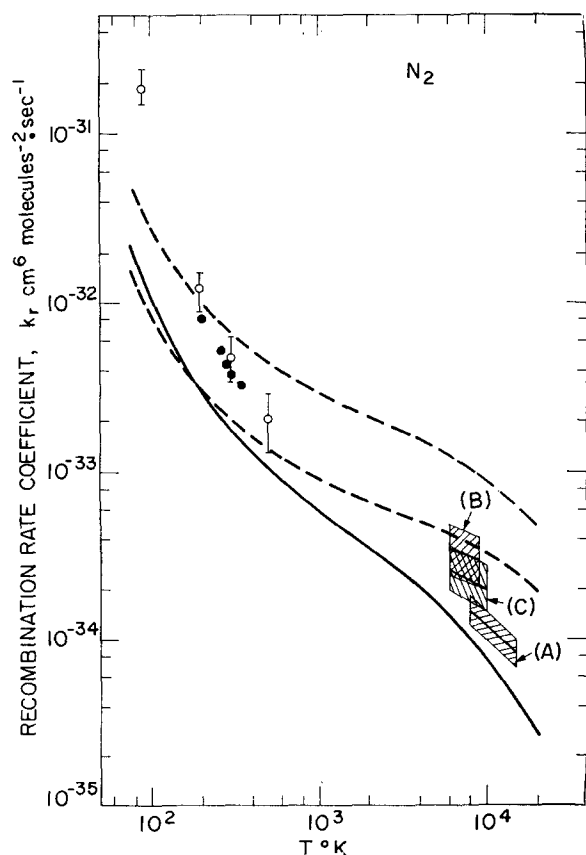


FIG. 7. Comparison between theoretical predictions of the recombination rate coefficient and experimental measurements as a function of  $T$ . Lower dashed curve:  $k_r^B(X^1\Sigma_g^+ | ^4S, ^4S)(N/N_0)$ ; upper dashed curve:  $[k_r^B(X^1\Sigma_g^+ | ^4S, ^4S) + k_r^B(A^3\Sigma_u^+ | ^4S, ^4S)](N/N_0)$ ; solid curve:  $[k_r(X^1\Sigma_g^+ | ^4S, ^4S) + k_r(A^3\Sigma_u^+ | ^4S, ^4S)]$ . The parameters  $U_{NAr}$ ,  $r_{eNAr}$ , and  $\beta_{NAr}$  were deduced using the empirical rules. O, Clyne and Stedman<sup>8</sup>; ●, Campbell and Thrush<sup>7</sup>; (A), Appleton *et al.*<sup>9</sup>; (B), Byron<sup>10</sup>; (C), Cary.<sup>20</sup>

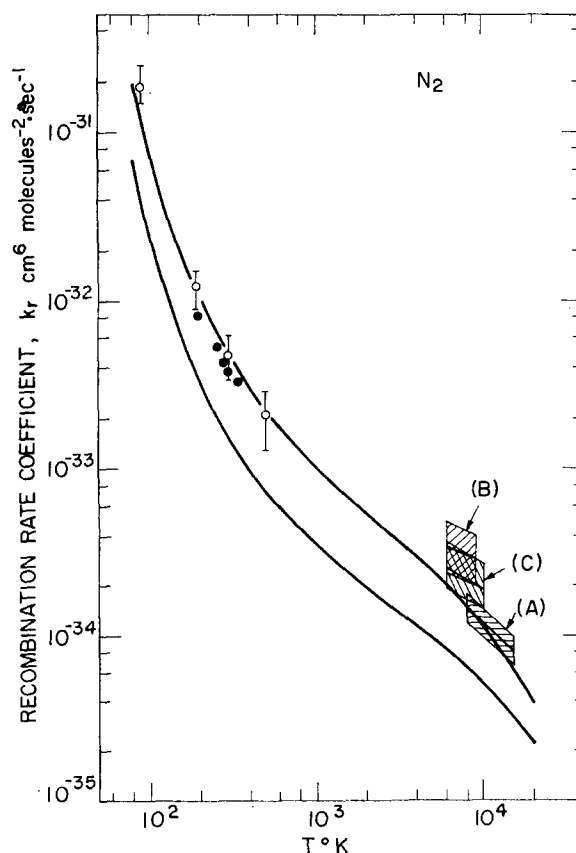


FIG. 8. Comparison between theoretical predictions of the recombination rate coefficient and experimental measurements as a function of  $T$ . Lower solid curve:  $k_r(X^1\Sigma_g^+ | ^4S, ^4S)$ ; upper solid curve:  $[k_r(X^1\Sigma_g^+ | ^4S, ^4S) + k_r(A^3\Sigma_u^+ | ^4S, ^4S)]$ . The well depth  $U_{NAr}$  was chosen so as to match the theory with the low-temperature experimental results. Remainder of legend same as Fig. 7.

It is apparent that the slope of the curve for  $[k_r(X^1\Sigma_g^+ | ^4S, ^4S) + k_r(A^3\Sigma_u^+ | ^4S, ^4S)]$  (solid curve in Fig. 7) does not match that of the low-temperature experimental results particularly well, and in fact, the theory grossly underestimates the recombination rate at 90°K.

A possible explanation for this disagreement is provided by the following considerations. We see from Eqs. (2.9) and (2.10) that  $k_r^B$  is roughly proportional to  $r_{eNAr}^2$  regardless of the temperature, and that at low temperatures, the major temperature variation of the rate coefficient is determined by the factor  $\exp(U_{NAr}/kT)$  (alterations in the value of  $\beta_{NAr}$  only affect the high-temperature rate significantly, i.e., increasing  $\beta_{NAr}$  makes the collisions more impulsive, thus increasing the rate at high temperatures). It would appear, therefore, that better agreement between experiment and theory may be obtained by increasing the well depth,  $U_{NAr}$ , somewhat beyond the value suggested by the empirical rule. The dependence of  $k_r^B$  on the factor  $\exp(U_{NAr}/kT)$  is equivalent to that which is obtained by invoking the "relaxed complex" mechanism,<sup>30-33</sup> and may be regarded as supplying further evidence to the claim that the phase-space theory is the most general theory and includes other more conventional reaction rate theories as special cases. (The phase-space theory in the form used tacitly assumes that the complex N·Ar is a "relaxed" complex, i.e., that it is present in its local equilibrium proportions.)

By assuming  $U_{NAr} \cong 380^\circ\text{K}$ , we recalculated  $k_r$  as a function of  $T$  as shown in Fig. 8, which again includes the experimental results for comparison. The upper full curve which passes through the experimental data is the sum of the recombination rate coefficients:  $k_r(X^1\Sigma_g^+ | ^4S, ^4S)$  and  $k_r(A^3\Sigma_u^+ | ^4S, ^4S)$ ; the lower curve illustrates the variation of  $k_r(X^1\Sigma_g^+ | ^4S, ^4S)$  alone. The agreement which is now obtained with the high-temperature dissociation measurements is also very good. To see this better, we have included an Arrhenius plot, Fig. 9, of these dissociation measurements<sup>9</sup> together with our own theoretical predictions for

$$k_d(X^1\Sigma_g^+ | ^4S, ^4S)$$

and

$$k_d(X^1\Sigma_g^+ | ^4S, ^4S) + k_d(A^3\Sigma_u^+ | ^4S, ^4S) \times Q(A^3\Sigma_u^+) / Q(X^1\Sigma_g^+).$$

Figures 8 and 9 show clearly that the rate coefficients for recombination and dissociation to and from the first excited state,  $A^3\Sigma_u^+$ , are about twice as large as those for recombination and dissociation to the ground state,  $X^1\Sigma_g^+$ . This is consistent with Campbell and Thrush's conclusion already discussed in Sec. III.A. Contributions from other excited states, i.e.,  $^5\Sigma_g^+$ ,  $^3\Delta_u$ ,  $B^3\Pi_g$ ,  $B'^3\Sigma_u^-$ ,  $a'^1\Sigma_u^-$ ,  $a^1\Pi_g$ , and  $W^1\Delta_u$ , have also been calculated, but they are all found to be

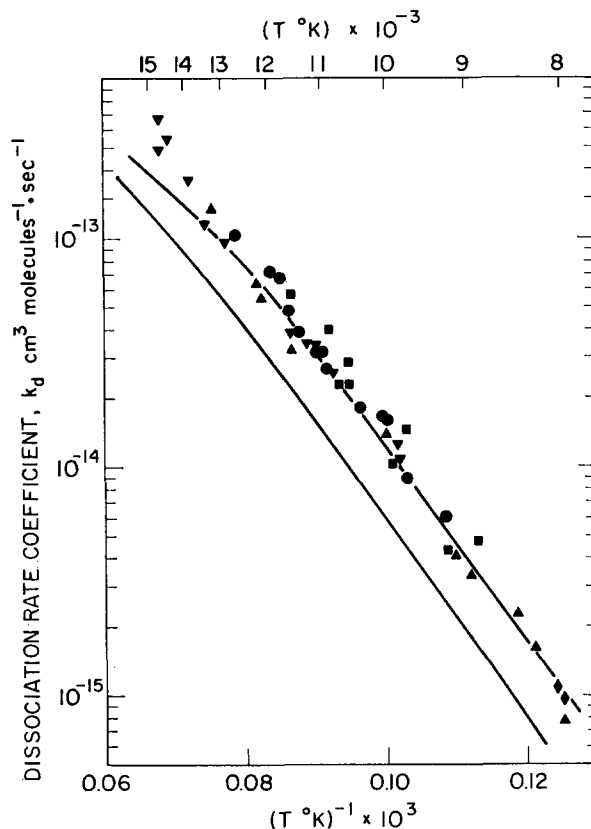
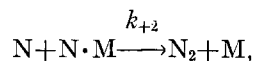
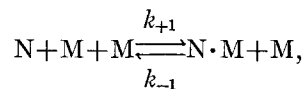


Fig. 9. Comparison between theoretical predictions of the dissociation rate coefficient and the experimental measurements taken from Appleton *et al.*<sup>9</sup> Lower solid curve:  $k_d(X^1\Sigma_g^+ | ^4S, ^4S)$ ; upper solid curve:  $[k_d(X^1\Sigma_g^+ | ^4S, ^4S) + k_d(A^3\Sigma_u^+ | ^4S, ^4S) \times Q(A^3\Sigma_u^+) / Q(X^1\Sigma_g^+)]$ .

negligible over the whole temperature range considered.

In view of our finding that  $U_{NAr} \cong 380^\circ\text{K}$ , we should, perhaps, question the assumption that N·Ar is a relaxed complex at low temperatures, particularly at 90°K. The kinetic scheme which describes the complex mechanism of recombination is



and for a relaxed complex, the condition

$$k_{-1}[N \cdot M][M] > k_{+2}[N \cdot M][N]$$

must be satisfied. Now in accordance with the simple collision theory for such reactions, we anticipate that

$$k_{-1}/k_{+2} \cong C \exp(-U_{NM}/kT),$$

where  $C$  is a constant of order unity. Thus, the condition for a relaxed complex reduces to

$$\exp(-U_{NM}/kT) > [N]/[M].$$

For  $U_{NM} \cong 380^\circ\text{K}$  and  $T = 90^\circ\text{K}$ , this indicates that the mole fraction of nitrogen atoms should be less than 1.4%, which we judge to be approximately true for Clyne and Stedman's lowest-temperature experiment. At room temperatures and above it is almost certainly true that the assumption of a relaxed complex is justified.

By making a small additional adjustment to  $U_{NAr}$  and to  $r_{NAr}$  and  $\beta_{NAr}$ , the theoretical value of  $k_r$  can be made to agree very closely with any given set of low- and high-temperature data. However, in view of the assumptions embodied in the theory and the remaining uncertainties of the experimental data, we do not believe that such a refinement is justified at this time.

## V. CONCLUSION

We have demonstrated that a modified phase-space trajectory calculation of the reaction rate coefficients is able to correlate both the very high- and the low-temperature dissociation and recombination rate measurements of nitrogen in argon.

Apart from the recognition that reaction progress via the first excited state of the molecule,  $A^3\Sigma_u^+$ , is important, the quantitative success of the theory is clearly dependent on prior knowledge of the interaction potential between nitrogen and argon atoms. However, from the results which we have presented here and preliminary results from a similar comparative investigation<sup>34</sup> which is being carried out in this laboratory on the dissociation and recombination of other diatomic molecules in argon (i.e.,  $\text{H}_2$ ,  $\text{O}_2$ ,  $\text{F}_2$ ,  $\text{Cl}_2$ ,  $\text{Br}_2$ ,  $\text{I}_2$ ,  $\text{HF}$ ,  $\text{HCl}$ ,  $\text{CO}$ , and  $\text{NO}$ ), we suggest that valid quantitative information on the interatomic potentials can be obtained from a proper synthesis of the phase-space theory and reliable experimental data obtained over a wide range of temperature. We make this suggestion in much the same spirit as Porter<sup>32</sup> chose to view the binding energy of the relaxed complex,  $\text{I}\cdot\text{M}$ , as an adjustable parameter for correlating iodine recombination measurements, and more recently, as Ip and Burns<sup>33</sup> similarly chose to view the binding energy of the relaxed complex,  $\text{Br}\cdot\text{M}$ , as an adjustable parameter for correlating their bromine recombination measurements. Such a view is, of course, entirely in keeping with existing methods which have been widely used for deducing intermolecular potential information at thermal energies from measurements of transport properties.

For those cases where the collision partners are highly reactive, e.g.,  $\text{X} + \text{X} + \text{X} \rightleftharpoons \text{X}_2 + \text{X}$ , the "dumbbell" model for the three-body interaction potential and the approximations used in deriving the expression for  $k_r^B$  [Eq. (2.9)] are no longer valid. A more realistic model for the interaction potential must be assumed and a more detailed analysis will be involved in the calculation. Work in this direction is being pursued at this laboratory on the  $(\text{H} + \text{H} + \text{H})$  system which,

hopefully, will shed some light on the question as to why, in dissociation and three-body recombination processes, the parent atoms are much more efficient third-body collision partners than those which are "inert."

\* This research was supported by the Advanced Research Projects Agency of the Department of Defense and was monitored by the Office of Naval Research under Contract No. N0014-67-A-0204-0040 and ARPA Order No. 322.

<sup>1</sup> N. B. Slater, *Theory of Unimolecular Reactions* (Cornell U. P., Ithaca, N.Y., 1959).

<sup>2</sup> S. Glasstone, K. Laidler, and H. Eyring, *The Theory of Rate Processes* (McGraw-Hill, New York, 1941).

<sup>3</sup> R. Fowler and E. A. Guggenheim, *Statistical Thermodynamics* (Cambridge U. P., Cambridge, England, 1952).

<sup>4</sup> J. C. Keck, *Advan. Chem. Phys.* **13**, 85 (1967).

<sup>5</sup> J. C. Keck, *J. Chem. Phys.* **32**, 1035 (1960).

<sup>6</sup> J. C. Keck and G. F. Carrier, *J. Chem. Phys.* **43**, 2284 (1965).

<sup>7</sup> I. M. Campbell and B. A. Thrush, *Proc. Roy. Soc. (London)* **A296**, 201 (1967).

<sup>8</sup> M. A. A. Clyne and D. H. Stedman, *J. Phys. Chem.* **71**, 3071 (1967).

<sup>9</sup> J. P. Appleton, M. Steinberg, and D. J. Liquornik, *J. Chem. Phys.* **48**, 599 (1968).

<sup>10</sup> C. A. Brau, J. C. Keck, and G. F. Carrier, *Phys. Fluids* **9**, 1885 (1966).

<sup>11</sup> In an earlier report version of this paper, Massachusetts Institute of Technology, Fluid Mechanics Lab. Rept. 70-2, February 1970, a Lennard-Jones (6-12) potential function was used to describe  $V_{\text{IM}}$ . In this paper the Morse form was used because we believe that it can more accurately describe the important repulsive part of the potential which is probably exponential in character.

<sup>12</sup> J. C. Keck, *Discussions Faraday Soc.* **33**, 173 (1962).

<sup>13</sup> A. I. Osipov and E. V. Stupochenko, *Usp. Fiz. Nauk* **79**, 81 (1963) [*Sov. Phys. Usp.* **6**, 47 (1963)].

<sup>14</sup> E. A. Mason and J. T. Vanderslice, *J. Chem. Phys.* **28**, 432 (1958).

<sup>15</sup> J. E. Jordan, S. O. Colgate, I. Amdur, and E. A. Mason, *J. Chem. Phys.* **52**, 1143 (1970).

<sup>16</sup> K. F. Herzfeld and T. A. Litovitz, *Absorption and Dispersion of Ultrasonic Waves* (Academic, New York, 1959).

<sup>17</sup> F. Kaufman, *Ann. Rev. Phys. Chem.* **20**, 45 (1969).

<sup>18</sup> M. Jeunehomme and A. B. F. Duncan, *J. Chem. Phys.* **41**, 1692 (1964).

<sup>19</sup> S. Byron, *J. Chem. Phys.* **44**, 1378 (1966).

<sup>20</sup> B. Cary, *Phys. Fluids* **8**, 26 (1965); **9**, 1047 (1966); K. L. Wray and S. Byron, *ibid.* **9**, 1046 (1966).

<sup>21</sup> A. R. Fairbairn, *J. Chem. Phys.* **48**, 515 (1968); A. R. Fairbairn, *Proc. Roy. Soc. (London)* **A312**, 207 (1969).

<sup>22</sup> J. P. Appleton, M. Steinberg, and D. J. Liquornik, *Bull. Am. Phys. Soc.* **13**, 1603 (1968); also, *J. Chem. Phys.* **52**, 2205 (1970).

<sup>23</sup> K. L. Wray, *J. Chem. Phys.* **44**, 623 (1966).

<sup>24</sup> We are grateful to Dr. K. L. Wray of Avco-Everett Res. Lab. for supplying us with his unpublished measurements of the "time-to-peak" intensity.

<sup>25</sup> R. B. Bernstein and J. T. Muckerman, *Advan. Chem. Phys.* **12**, 389 (1967).

<sup>26</sup> J. T. Waber and D. T. Cromer, *J. Chem. Phys.* **42**, 4116 (1965).

<sup>27</sup> J. C. Slater, *J. Chem. Phys.* **41**, 3199 (1964).

<sup>28</sup> H. S. Johnston, *J. Am. Chem. Soc.* **86**, 1643 (1964).

<sup>29</sup> F. R. Gilmore, *J. Quant. Spectry. Radiative Transfer* **5**, 369 (1965).

<sup>30</sup> O. K. Rice, *J. Chem. Phys.* **9**, 258 (1941).

<sup>31</sup> D. L. Bunker and N. Davidson, *J. Am. Chem. Soc.* **80**, 5085 (1958).

<sup>32</sup> G. Porter, *Discussions Faraday Soc.* **33**, 198 (1962).

<sup>33</sup> J. K. K. Ip and G. Burns, *J. Chem. Phys.* **51**, 3414 (1969).

<sup>34</sup> V. H. Shui, J. P. Appleton, and J. C. Keck, "The Dissociation and Recombination of Diatomic Molecules; Comparisons Between Experiment and Theory," Massachusetts Institute of Technology, Fluid Mechanics Lab. Rept. 70-3, April 1970. To be presented at the Thirteenth Symposium (International) on Combustion, University of Utah, 23-29 August 1970.